Response and resistance to MEK inhibition in leukaemias initiated by hyperactive Ras

Jennifer O. Lauchle[1], Doris Kim[1], Doan T. Le[1], Keiko Akagi[5], Michael Crone[1], Kimberly Krisman[1], Kegan Warner[1], Jeannette M. Bonifas[1], Qing Li[2], Kristen M. Coakley[3], Ernesto Diaz-Flores[1], Matthew Gorman[1], Sally Przybranowski[6], Mary Tran[1], Scott C. Kogan[4], Jeroen P. Roose[3], Neal G. Copeland[7], Nancy A. Jenkins[7], Luis Parada[8], Linda Wolff[9], Judith Sebolt-Leopold[6] & Kevin Shannon[1]

The cascade comprising Raf, mitogen-activated protein kinase kinase (MEK) and extracellular signal-regulated kinase (ERK) is a therapeutic target in human cancers with deregulated Ras signalling, which includes tumours that have inactivated the *Nf1* tumour suppressor[1,2]. *Nf1* encodes neurofibromin, a GTPase-activating protein that terminates Ras signalling by stimulating hydrolysis of Ras–GTP. We compared the effects of inhibitors of MEK in a myeloproliferative disorder (MPD) initiated by inactivating *Nf1* in mouse bone marrow and in acute myeloid leukaemias (AMLs) in which cooperating mutations were induced by retroviral insertional mutagenesis. Here we show that MEK inhibitors are ineffective in MPD, but induce objective regression of many *Nf1*-deficient AMLs. Drug resistance developed because of outgrowth of AML clones that were present before treatment. We cloned clone-specific retroviral integrations to identify candidate resistance genes including *Rasgrp1*, *Rasgrp4* and *Mapk14*, which encodes p38α. Functional analysis implicated increased RasGRP1 levels and reduced p38 kinase activity in resistance to MEK inhibitors. This approach represents a robust strategy for identifying genes and pathways that modulate how primary cancer cells respond to targeted therapeutics and for probing mechanisms of *de novo* and acquired resistance.

Aberrant Ras signalling contributes to the pathogenesis of myeloid malignancies and can result from acquired *RAS* mutations or from alternative genetic mechanisms that include *FLT3* internal tandem duplications, the *BCR–ABL* fusion, *PTPN11* mutations and *NF1* inactivation (reviewed in ref. 3). Children with neurofibromatosis type 1 (NF1) have a 200- to 500-fold excess incidence of juvenile myelomonocytic leukaemia, an aggressive MPD characterized by leukocytosis, splenomegaly and tissue infiltration (reviewed in ref. 4). The bone marrows of affected patients frequently show loss of the normal parental *NF1* allele and elevated ERK activity[5–7]. Bi-allelic inactivation of murine *Nf1* causes an MPD in *Mx1-Cre, Nf1^flox/flox* mice that closely models juvenile myelomonocytic leukaemia[8].

We injected the MOL4070LTR retrovirus[9] into *Mx1-Cre, Nf1^flox/flox* pups to identify genes and pathways that might cooperate with *Nf1* inactivation to induce progression of MPD to AML[3]. These mice developed acute leukaemia sooner and at a higher rate than control *Mx1-Cre*-negative littermates that retain normal *Nf1* function (Fig. 1a). *Nf1*-deficient AMLs are highly aggressive (Fig. 1b, c), show variable expression of myeloid surface markers, are transplantable into sublethally irradiated recipients and form cytokine-dependent blast colonies in methylcellulose cultures.

The MEK inhibitor CI-1040 (ref. 10) reduced the growth of myeloid progenitor colonies from the bone marrows of *Mx1-Cre, Nf1^flox/flox* mice with MPD and wild-type controls to a similar extent (Fig. 1d). By contrast, blast colony growth from many *Nf1*-deficient AMLs was exquisitely sensitive, with abrogation of colony growth at 10- to 100-fold lower drug concentrations (Fig. 1d). These *in vitro* data suggested that cooperating mutations render *Nf1*-mutant AMLs more dependent on Raf/ERK/MEK signalling. To pursue this question, we first determined the maximally tolerated dose of CI-1040 to be 100 mg kg⁻¹ twice daily in wild-type mice, collected bone marrow at defined time points after a single drug dose, and showed that CI-1040 treatment transiently reduced the ability of granulocyte–macrophage
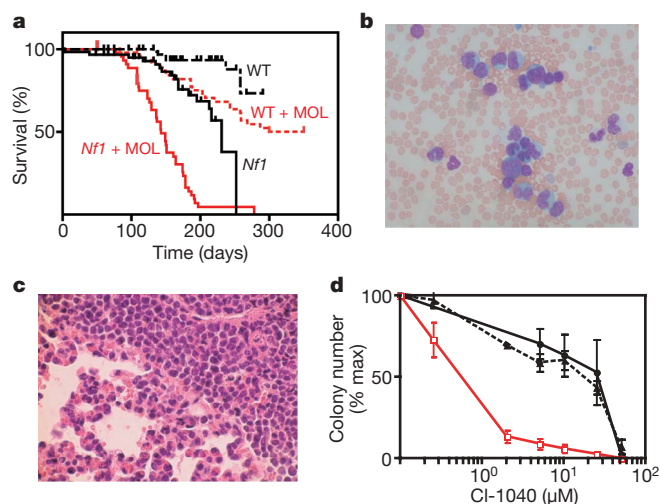

Figure 1 | Retroviral mutagenesis induces AML in *Mx1-Cre, Nf1^flox/flox* mice and alters response to MEK inhibition. a, *Mx1-Cre, Nf1^flox/flox* mice that were infected with MOL4070LTR (*Nf1* + MOL; *n* = 47) had markedly reduced survival compared with control littermates that received this virus (wild type + MOL; *n* = 49; *P* < 0.0001). Survival curves for *Mx1-Cre, Nf1^flox/flox* (*Nf1*) and wild-type mice that were not injected with MOL4070LTR are also shown. **b, c**, Myeloblasts in the peripheral blood (**b**) and infiltrating into lung tissues (**c**) of *Mx1-Cre, Nf1^flox/flox* mice with AML. **d**, Myeloid colony growth from the bone marrows of wild-type mice (filled circles, *n* = 12) *Mx1-Cre, Nf1^flox/flox* mice with MPD (filled triangles, *n* = 6), and *Mx1-Cre, Nf1^flox/flox* mice with AML (open squares, *n* = 8) over a range of CI-1040 concentrations (log scale). Colony growth was assayed in the presence of a saturating concentration of GM-CSF. Error bars, s.e.m.

[1]Department of Pediatrics, [2]Department of Medicine, [3]Department of Anatomy, [4]Department of Laboratory Medicine, University of California, San Francisco, California 94143, USA. [5]Mouse Cancer Genetics Program, National Cancer Institute, Fredrick, Maryland 21702, USA. [6]Pfizer Global Research and Development, Ann Arbor, Michigan 48105, USA. [7]Institute of Molecular and Cell Biology, Singapore 138673, Singapore. [8]University of Texas Southwestern, Dallas, Texas 75235, USA. [9]Laboratory of Cellular Oncology, National Cancer Institute, National Institutes of Health, Bethesda, Maryland 20892, USA.

colony-stimulating factor (GM-CSF) to increase phosphorylated ERK levels (Supplementary Fig. 1a). We then treated control or *Mx1-Cre, Nf1^{flox/flox}* mice with MPD for 28 days ($n = 5$ per group). Consistent with the *in vitro* data, CI-1040 had no beneficial therapeutic index in mice with MPD (Supplementary Fig. 1b, c and data not shown). Biochemical analysis of bone marrow obtained 2–8 h after the 56th and final dose of CI-1040 revealed reduced ERK phosphorylation that was similar to the responses of wild-type mice that received a single drug dose (Supplementary Fig. 1a, d).

To investigate the unexpected *in vitro* sensitivity of *Nf1* mutant AMLs to CI-1040, we transplanted four independent leukaemias into 23 recipients. Mice with AML blasts in the peripheral blood were assigned to treatment with either vehicle ($n = 11$) or CI-1040 ($n = 12$) at the same dose and schedule that was ineffective in the MPD. CI-1040 treatment induced rapid and extensive reductions in blood leukocyte counts (Fig. 2a), with clearance of blasts and reappearance of normal neutrophils (data not shown). Survival increased greater than threefold (Fig. 2b). However, recipients of *Mx1-Cre, Nf1^{flox/flox}* AMLs invariably died with recurrent leukaemia despite ongoing treatment (Fig. 2b). These relapsed AMLs had similar morphological and immunophenotypic features as the parental leukaemias, but demonstrated *in vitro* resistance to MEK inhibitors and were refractory to treatment in secondary recipients (Fig. 2c and data not shown). Sensitive AMLs showed a greater reduction in 5′-bromodeoxyuridine incorporation after CI-1040 exposure than either wild-type or resistant leukaemia cells (Supplementary Fig. 2). We also exposed pairs of sensitive and resistant AMLs to CI-1040 *in vitro* to ask if resistance is associated with reactivation of MEK. Importantly, ERK phosphorylation in response to GM-CSF was inhibited at the same concentration of CI-1040 (Fig. 2d, e).
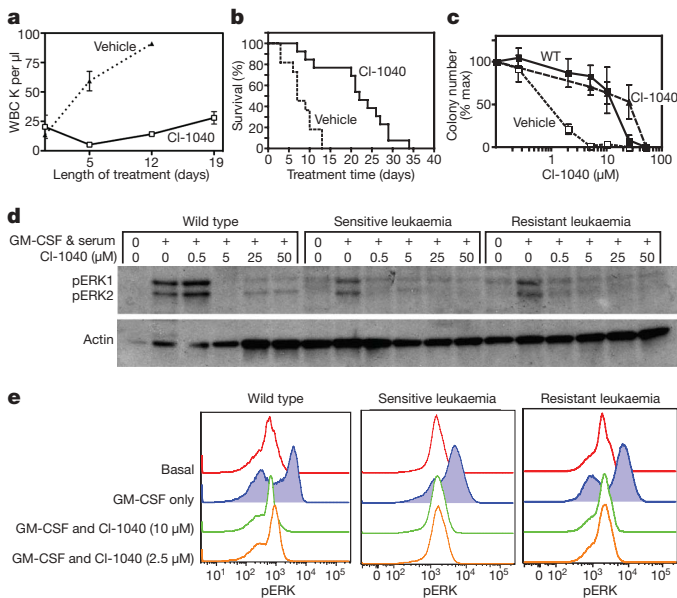
PD0325901 is a MEK inhibitor with more favourable pharmacological characteristics than CI-1040 (ref. 11). We defined a maximally tolerated dose of 12.5 mg kg^{-1} d^{-1} for PD0325901, and found that doses greater than 5 mg kg^{-1} d^{-1} reduced ERK activation in response to GM-CSF for 24 h (Supplementary Fig. 3a). To ask if prolonging the duration of MEK inhibition affects drug response and resistance *in vivo*, we administered PD0325901 to mice that were transplanted with two AMLs from the CI-1040 trial (AMLs 6554 and 6537). Recipients that received PD0325901 demonstrated the same pattern of response, relapse and overall survival (Supplementary Fig. 3b). We also tested two other *Nf1*-deficient AMLs for response to PD0325901. AML 7723 was less sensitive to MEK inhibition in methylcellulose cultures, and administering PD0325901 to recipient mice neither prolonged survival nor changed the half-maximal inhibitory concentration (IC$_{50}$) for blast colony formation (Supplementary Fig. 4). AML 7710 showed an *in vitro* response to PD0325901 that was similar to sensitive leukaemias; however, *in vivo* treatment did not prolong survival or select for clones with altered drug responsiveness (Supplementary Fig. 4). Together, these studies define a heterogeneous response of *Nf1*-deficient AMLs to MEK inhibition.

Digesting DNA from AML 6554 with restriction enzymes and Southern blot analysis with a MOL4070LTR-specific probe revealed clonal evolution of the resistant leukaemia (Fig. 3a). To identify candidate genes that might influence response to CI-1040, we exploited a shotgun cloning strategy[12] to characterize MOL4070LTR integrations. Sensitive parental AML 6554 and resistant leukaemias from CI-1040- and PD0325901-treated recipient mice shared some common integrations as well as unique insertions (Fig. 3a and Supplementary Table 1). Importantly, resistant leukaemias from independent recipients that were treated with CI-1040 or PD0325901 invariably showed the same integration patterns (Fig. 3a and Supplementary Table 1). These data and the rapid emergence of resistance imply that resistant subclones that are present within the initial AML are selected *in vivo* during MEK inhibitor treatment.

The patterns of MOL4070LTR integrations in sensitive and resistant AML 6554 suggested that *Rasgrp* genes might contribute to drug resistance (Supplementary Table 1). We developed quantitative real-time PCR (rtPCR) assays to correlate *Rasgrp1* insertion copy number and RNA expression in AML 6554 with the integration data shown in Supplementary Table 1. Whereas analysis of sensitive AML 6554 from eight independent recipients revealed only low levels of a unique integration junction fragment, four independent PD0325901-resistant leukaemias demonstrated 1,000-fold (range 500- to 1,500-fold) increases in DNA copy number. Similarly, *Rasgrp1* messenger RNA levels were increased an average of tenfold (range 6.5- to 19-fold) in resistant compared with sensitive leukaemias (Fig. 3b). RasGRP proteins stimulate guanine nucleotide exchange on Ras, which increases Ras–GTP levels (reviewed in ref. 13). We reasoned that increased *Rasgrp1* expression might result in elevated Ras–GTP levels in resistant AML 6554. Indeed, whereas basal Ras–GTP levels were low in the parental leukaemia and returned to baseline 60 min after exposure to GM-CSF, we observed constitutive Ras activation in the resistant AML (Fig. 3c). Resistant AML 6554 also formed cytokine-independent blast colonies in methylcellulose (Fig. 3d). This observation is consistent with biochemical and computational analyses in lymphocytes, which predict that Ras signalling becomes independent of receptor input when RasGRP levels are elevated[14]. To assess the functional importance of *Rasgrp1* overexpression in resistant AML 6554 further, we infected the sensitive and resistant leukaemias with a lentiviral vector encoding both a short hairpin RNA (shRNA) that efficiently reduces RasGRP1 protein (Supplementary Fig. 5) and a green fluorescent protein (GFP) marker. GFP-positive cells were isolated by sorting and plated in methylcellulose medium containing GM-CSF and a range of PD0325901 concentrations. Neither the *Rasgrp1* shRNA virus nor a control virus altered the sensitivity of parental AML blast colony forming cells to the MEK inhibitor (Fig. 3e). By contrast, infecting resistant AML 6554 with the *Rasgrp1* shRNA lentivirus restored the sensitivity
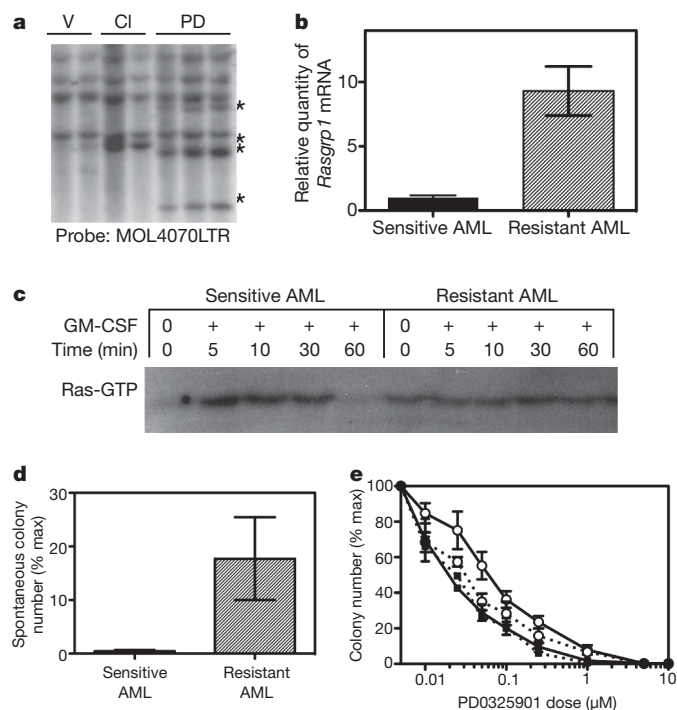

Figure 2 | **Response and resistance to CI-1040 in *Mx1-Cre, Nf1^{flox/flox}* mice with AML. a,** Leukocyte counts were markedly decreased in mice treated with CI-1040 ($n = 13$) compared with the vehicle ($n = 12$). Error bars, s.e.m. **b,** Survival was prolonged by approximately threefold in mice that received CI-1040 (odds ratio 3.1; confidence interval (CI) 2.7–3.6; $P < 0.0001$). **c,** Myeloid colony growth from the bone marrows of mice with recurrent leukaemia are less sensitive to CI-1040 inhibition than the parental AMLs. Colony growth in methylcellulose is compared for wild-type bone marrow (filled squares, $n = 2$), for primary AML cells harvested from vehicle-treated mice (open squares, $n = 4$) and for AML cells obtained after relapse in recipients that were treated with CI-1040 (filled triangles, $n = 3$). Error bars, s.e.m. **d, e,** CI-1040 abrogates the ability of GM-CSF to stimulate ERK phosphorylation in both sensitive and resistant AMLs as assessed by western blotting (**d**) or phospho-flow cytometry (**e**).

2

Figure 3 | Genetic and functional analysis implicates *Rasgrp1* overexpression as a resistance mechanism in AML 6554. a, Retroviral integrations in DNA samples from AML 6554 in independent mice after treatment with vehicle (V), CI-1040 (CI) or PD0325901 (PD). Stars denote restriction fragments that are present in resistant AMLs, but are not seen in the sensitive parental leukaemia. **b,** Quantitative PCR analysis of *Rasgrp1* expression in sensitive and resistant AML 6554 ($n = 3$ in each group, mean with s.d., $P < 0.002$ Student's *t*-test). **c,** Ras-GTP levels in AML 6554 show constitutive activation in the resistant leukaemia. **d,** Resistant AML 6554 demonstrates substantial cytokine-independent blast colony growth ($n = 5$), which is not seen in the sensitive leukaemia ($n = 6$) ($P = 0.0350$, *t*-test). **e,** Resistant AML 6554 that is infected with a *Rasgrp1* shRNA (open circles, dotted line, $n = 7$) demonstrates an $IC_{50} = 0.03$ μM (95% CI 0.02–0.03), which is significantly lower than the IC_{50} of resistant cells infected with the control vector ($IC_{50} = 0.06$ μM, 95% CI 0.05–0.07; open circles, solid line, $n = 7$). The IC_{50} of parental sensitive AML infected with shRNA vector to *Rasgrp1* ($IC_{50} = 0.02$ μM, 95% CI 0.017–0.024; filled squares, dotted line, $n = 3$) or control vector ($IC_{50} = 0.02$ μM, 95% CI 0.017–0.028; filled squares, solid line $n = 3$) are not statistically significantly different than resistant AML 6554 infected with *Rasgrp1* shRNA. Error bars, s.e.m. in **d** and **e**.

of these cells to PD0325901, with a shift of the IC_{50} into the same range as in the sensitive parental AML (Fig. 3e).

Multiple recipients that were transplanted with AML 6537 relapsed with the same resistant clone after treatment with either CI-1040 or PD0325901 (Fig. 4a). This resistant leukaemia showed a distinct retroviral integration pattern, including one within *Mapk14*, which encodes p38α (Supplementary Table 2). rtPCR of proviral/host DNA junctions confirmed that the inserted allele copy number is increased 1,000-fold (range 1,000- to 10,000-fold) in the resistant AML. The proviral insertion is in the anti-sense orientation, and Southern blot analysis supports inactivation of one *Mapk14* allele (Fig. 4a, b). Consistent with this prediction, basal p38 kinase activity is reduced in resistant AML 6537 (Fig. 4c). To investigate further whether decreased p38α activity modulates resistance to MEK inhibitors in primary leukaemia cells, we enumerated blast colonies from AML 6537 in the presence of either CI-1040, SB202190 (a specific inhibitor of p38α)[15,16] or both drugs. SB202190 strongly antagonized the inhibitory effects of CI-1040 on the sensitive leukaemia, but had minimal effects on the resistant AML (Fig. 4d).

Cooperating mutations that induce progression of MPD to AML render these more aggressive leukaemias highly dependent upon
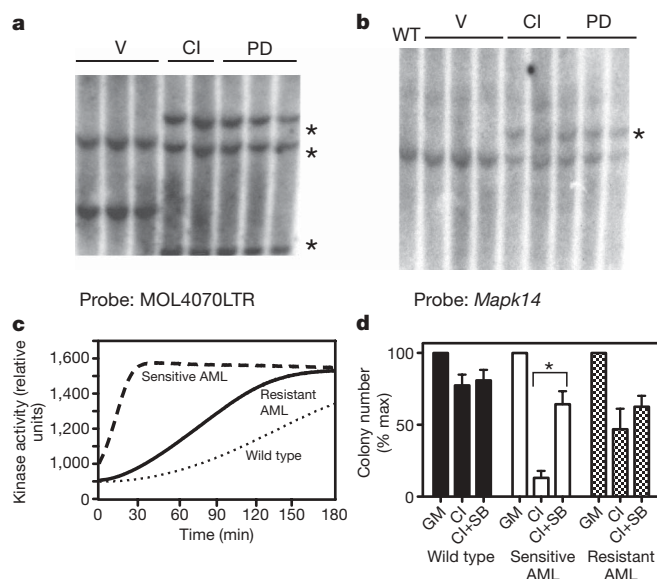

Figure 4 | Genetic and functional analysis of AML 6537 associates reduced p38α kinase activity with resistance to MEK inhibition. a, Southern blot analysis of MOL4070LTR integrations of AML 6537 after treatment with vehicle (V), CI-1040 (CI) or PD0325901 (PD). Stars denote restriction fragments that are present in all the resistant AMLs, but are not seen in the sensitive leukaemia. **b,** Southern blot analysis of paired sensitive and resistant AML 6537 with a *Mapk14* probe. The resistant leukaemias shown in lanes CI and PD show a *Mapk14* hybridization fragment, which overlaps with one of the MOL4070LTR bands in the resistant leukaemias shown in **a. c,** Basal p38 kinase activity of resistant AML 6537 cells (solid line) is reduced compared with the parental leukaemia (dashed line), but remains elevated above wild-type bone marrow cells (dotted line). This is a representative example of three independent experiments. **d,** SB202190 (SB), a p38α inhibitor, antagonizes the ability of CI-1040 (CI) to reduce blast colony inhibition in parental AML 6537 (white bars, $n = 7$) in the presence of GM-CSF (GM). Blast colony growth of sensitive AML 6537 is significantly increased by the addition of SB to CI-1040 (*$P = 0.0043$; unpaired *t*-test). By contrast, CI-1040 (2.5 μM) has a inhibitory effect on wild-type CFU-GM colony (black bars, $n = 8$) and resistant AML 6537 (hatched bars, $n = 5$) blast colony growth, which is not affected by 2.5 μM SB202190. Error bars, s.e.m.

MEK for proliferation and survival. The transient remissions induced by imatinib in advanced ('blast crisis') CML[17] are remarkably similar to the responses of *Mx1-Cre, Nf1^flox/flox* AMLs to MEK inhibition. Relapse of blast crisis CML and of *Nf1*-mutant murine leukaemias is due to outgrowth of a minor population of drug-resistant cells that is present before treatment with targeted agents[18]. Similarly, 'back-tracking' experiments in acute lymphoblastic leukaemias showed that the dominant clone at relapse is frequently detectable before treatment[19]. Relapsed acute lymphoblastic leukaemia clones differ from the predominant clone at diagnosis by a few genetic changes[20]. Diverse mutations of genes involved in lymphoid developmental programs, cell cycle control and DNA damage responses are enriched in drug-resistant clones, whereas alterations in drug import, export or metabolism are relatively uncommon[20]. Understanding how pre-existing drug-resistant clones underlie cancer relapse has fundamental implications for developing better therapeutic strategies.

As MEK is one component of a complex network of Ras effectors, it is possible to envision multiple mechanisms of acquired resistance. Our data support this idea. A provocative implication of our studies of AML 6554 showing that *Rasgrp1* overexpression modulates the response to MEK inhibitors is that globally increasing Ras–GTP levels can overcome the effects of inhibiting a major Ras effector in some cancers. We implicated reduced p38 kinase activity as an alternative mechanism of MEK resistance in AML 6537. Interestingly, cancer cell lines that undergo apoptosis in response to oncoprotein inhibition show a rapid decrease in phosphorylated ERK followed by an increase

in phosphorylated p38 levels[21]. As *Nf1*-deficient AMLs have elevated basal p38 kinase activity, our studies suggest that inhibiting onco-genic Raf–MEK–ERK signalling results in unopposed p38 kinase activity, which contributes to cell death. This general idea is consistent with the observation that p38 inhibitors induce imatinib resistance in cultured CML cells[21,22].

The AMLs that we have characterized so far showed diverse retro-viral integrations (Supplementary Tables 1–3), and comprehensive genetic and preclinical analyses are required to uncover the full spectrum of mutations associated with drug resistance. Despite this limitation, a broad implication of our data is that cell lineage, the nature of cooperating mutations and the order in which they are acquired in specific cancers will modulate the efficacy of targeted inhibitors of Ras effector pathways. Insertional mutagenesis in genetically accurate mouse cancer models is a powerful tool for dissecting the molecular basis of cellular responses to oncogenic stress and for uncovering genes that contribute to drug sensitivity and resistance.

METHODS SUMMARY

Inhibitors. CI-1040 and PD0325901 (Pfizer) were administered as described in Supplementary Methods. SB202190 (Calbiochem) was diluted in 100% dimethylsulphoxide.

Mouse strains and retroviral insertional mutagenesis: mice. All procedures involving mice were approved by the UCSF Committee on Animal Research. MOL4070LTR stocks were prepared as described[6]. Mice received a single intra-peritoneal injection containing 10^5 viral particles in 100 μl admixed with 500 μg of pI-pC (to activate *Mx1-Cre* expression) between days 3 and 5 of life. Mice with leukaemia were killed and bone marrow was cryopreserved. Leukaemias were classified based on established morphological and flow cytometric criteria[23].

Adoptive transfer and treatment. Cryopreserved AMLs were injected intravenously (10^6 cells per mouse) into 6- to 8-week-old recipient mice that received a single radiation dose of 450 cGy. Recipients with leukaemic cells in the peripheral blood were randomly assigned to receive either CI-1040/PD0325901 or control vehicle. Mice were weighed weekly to adjust the drug dose, observed daily and killed when they became moribund or on the 28th day of treatment.

Myeloid progenitor growth and pharmacodynamics studies. CFU-GM and blast colonies were grown in methylcellulose medium M3231 (Stem Cell Technologies) and scored by indirect microscopy. MEK inhibition was assessed by stimulating bone marrow cells with GM-CSF and then measuring phosphorylated ERK levels by western blotting (see also Supplementary Methods).

Retroviral integrations and quantitative rtPCR. Junction fragments corresponding to retroviral integrations were identified as described[24]. PCR primers were designed to detect integration junctions[25] (see also Supplementary Methods).

p38 kinase assay. Kinase activity of mice was quantified in 100-μg lysates with the Omnia Plate IP kit (BioSource), in which activation of a MAPKAPK2 evokes a change in fluorescent properties owing to chelation-enhanced fluorophore. A fluorescent plate reader in real-time kinetic mode quantified p38 kinase activities.

Full Methods and any associated references are available in the online version of the paper at www.nature.com/nature.

1. Downward, J. Targeting RAS signalling pathways in cancer therapy. *Nature Rev. Cancer* 3, 11–22 (2003).
2. Schubbert, S., Shannon, K. & Bollag, G. Hyperactive Ras in developmental disorders and cancer. *Nature Rev. Cancer* 7, 295– 308 (2007).
3. Van Etten, R. A. & Shannon, K. M. Focus on myeloproliferative diseases and myelodysplastic syndromes. *Cancer Cell* 6, 547–552 (2004).
4. Lauchle, J. O., Braun, B. S., Loh, M. L. & Shannon, K. Inherited predispositions and hyperactive Ras in myeloid leukemogenesis. *Pediatr. Blood Cancer* 46, 579–585 (2006).
5. Shannon, K. M. et al. Loss of the normal NF1 allele from the bone marrow of children with type 1 neurofibromatosis and malignant myeloid disorders. *N. Engl. J. Med.* 330, 597–601 (1994).
6. Bollag, G. et al. Loss of *NF1* results in activation of the Ras signaling pathway and leads to aberrant growth in murine and human hematopoietic cells. *Nature Genet.* 12, 144–148 (1996).
7. Side, L. et al. Homozygous inactivation of the NF1 gene in bone marrow cells from children with neurofibromatosis type 1 and malignant myeloid disorders. *N. Engl. J. Med.* 336, 1713–1720 (1997).
8. Le, D. T. et al. Somatic inactivation of Nf1 in hematopoietic cells results in a progressive myeloproliferative disorder. *Blood* 103, 4243–4250 (2004).
9. Wolff, L., Koller, R., Hu, X. & Anver, M. R. A Moloney murine leukemia virus-based retrovirus with 4070A long terminal repeat sequences induces a high incidence of myeloid as well as lymphoid neoplasms. *J. Virol.* 77, 4965–4971 (2003).
10. Sebolt-Leopold, J. S. et al. Blockade of the MAP kinase pathway suppresses growth of colon tumors *in vivo*. *Nature Med.* 5, 810–816 (1999).
11. Brown, A. P., Carlson, T. C., Loi, C. M. & Graziano, M. J. Pharmacodynamic and toxicokinetic evaluation of the novel MEK inhibitor, PD0325901, in the rat following oral and intravenous administration. *Cancer Chemother. Pharmacol.* 59, 671–679 (2007).
12. Dupuy, A. J. et al. Mammalian mutagenesis using a highly mobile somatic Sleeping Beauty transposon system. *Nature* 436, 221–226 (2005).
13. Stone, J. C. Regulation of Ras in lymphocytes: get a GRP. *Biochem. Soc. Trans.* 34, 858–861 (2006).
14. Das, J. et al. Digital signaling and hysteresis characterize ras activation in lymphoid cells. *Cell* 136, 337–351 (2009).
15. Bain, J. et al. The selectivity of protein kinase inhibitors: a further update. *Biochem. J.* 408, 297–315 (2007).
16. Fabian, M. A. et al. A small molecule-kinase interaction map for clinical kinase inhibitors. *Nature Biotechnol.* 23, 329–336 (2005).
17. Druker, B. J. et al. Activity of a specific inhibitor of the BCR-ABL tyrosine kinase in the blast crisis of chronic myeloid leukemia and acute lymphoblastic leukemia with the Philadelphia chromosome. *N. Engl. J. Med.* 344, 1038–1042 (2001).
18. Shah, N. P. et al. Multiple BCR-ABL kinase domain mutations confer polyclonal resistance to the tyrosine kinase inhibitor imatinib (STI571) in chronic phase and blast crisis chronic myeloid leukemia. *Cancer Cell* 2, 117–125 (2002).
19. Choi, S. et al. Relapse in children with acute lymphoblastic leukemia involving selection of a preexisting drug-resistant subclone. *Blood* 110, 632–639 (2007).
20. Mullighan, C. G. et al. Genomic analysis of the clonal origins of relapsed acute lymphoblastic leukemia. *Science* 322, 1377–1380 (2008).
21. Sharma, S. V. et al. A common signaling cascade may underlie 'addiction' to the Src, BCR-ABL, and EGF receptor oncogenes. *Cancer Cell* 10, 425–435 (2006).
22. Parmar, S. et al. Role of the p38 mitogen-activated protein kinase pathway in the generation of the effects of imatinib mesylate (STI571) in BCR-ABL-expressing cells. *J. Biol. Chem.* 279, 25345–2532 (2004).
23. Kogan, S. C. et al. Bethesda proposals for classification of nonlymphoid hematopoietic neoplasms in mice. *Blood* 100, 238–245 (2002).
24. Akagi, K. et al. RTCGD: retroviral tagged cancer gene database. *Nucleic Acids Res.* 32 (Database issue), D523–D527 (2004).
25. Curtiss, N. P. et al. Isolation and analysis of candidate myeloid tumor suppressor genes from a commonly deleted segment of 7q22. *Genomics* 85, 600–607 (2005).

METHODS

Preparation and administration of MEK inhibitors. CI-1040 and PD0325901 were dissolved in 100% DMSO for *in vitro* assays and suspended in 0.5% hydroxypropyl methylcellulose and 0.2% Tween 80 for administration to mice. For intraperitoneal injection of mice, 100 mg kg^{-1} of CI-1040 was in a volume 100–150 µl and a concentration of 30 mg ml^{-1}. PD0325901 was administered in 150–200 µl volume by oral gavage (OG) to achieve doses of 2.5, 5.0, 7.5, 10.0 and 12.5 mg kg^{-1}.

Proliferation assay. Cells were plated in 6 ml of IMDM 20% FBS with a saturating dose of 2 ng µl^{-1} of GM-CSF at a density no greater than 2×10^6 cells per millilitre and incubated with 10 µM of CI-1040 or 0.2% DMSO for 22 h at 37 °C and 5% CO$_2$. Cells were pulsed with 5-bromo-2-deoxyuridine (BrdU) (BD Pharmingen FITC BrdU Flow Kit) and left to incorporate for 2 h. Cells were harvested from wells and washed with HBSS and 2% heat-inactivated FBS. Cells were treated with DNase to expose incorporated BrdU and stained with FITC conjugated anti-BrdU. Total intracellular DNA was stained with 7-AAD and samples were collected on a multicolour flow cytometer (LSR II) with a minimum of 10,000 total events.

GM-CSF stimulation and ERK phosphorylation. Femoral bone marrow cells were collected into 0.1% serum without growth factors. After 15 min, the cells were stimulated with 0 or 10 ng ml^{-1} of GM-CSF and 0 or 10% fetal bovine serum for 10 min. The cells were washed once with PBS and lysed in 25 mM HEPES, pH 7.5, 150 mM NaCl, 1% NP-40, 0.25% Na deoxycholate, 10% glycerol, 10 mM MgCl$_2$, 25 mM NaF, 1 mM Na orthovanadate and Complete protease inhibitors (Amersham). Protein concentrations were quantitated and equalized for loading using the Bio-Rad protein assay (Bio-Rad). Samples were boiled for 5 min in 1 × Laemmli buffer, run on a 10% Tris-HCl Criterion Precast Gel (Bio-Rad) and transferred onto a nitrocellulose membrane. The membranes were blocked in TBS-Tween containing 5% milk for 1 h or in 5% BSA overnight before incubation at 4 °C with antiphospho-ERK 1/2 (1:1,000), anti-ERK (1:1,000) and anti-actin (1:500) (Cell Signaling Technologies). The blots were developed with a horseradish-peroxidise-conjugated secondary anti-rabbit antibody (Amersham). Proteins were visualized by enhanced chemiluminescence (Amersham).

Restriction digestion and Southern blotting. Bone marrow or spleen DNA from leukaemia mice was cut with HindIII, separated on an agarose gel, transferred onto a nylon membrane and hybridized overnight with a ^{32}P-labelled fragment of 4070LTR or *Mapk14*.

Cloning and bioinformatic analysis of viral insertions. Approximately 1 µg of genomic DNA was digested with NlaIII (IRDRR) or MseI and purified using a Qiagen column (QIAquick PCR purification). A 5-µl aliquot was added to a ligation reaction containing 150 µM of a double- stranded linker. Linkers were generated by annealing equimolar amounts of NlaIII linker+ (5′-GTAATAC GACTCACTATAGGGCTCCGCTTAAGGGACCATG-3) and NlaIII linker− (5′-/5Phos/GTCCCTTAAGCGGAG/3SpacerC3/-3′) or MseI linker+ (5′-GTA ATACGACTCACTATAGGGCTCCGCTTAAGGGAC-3′) and MseI linker− (5′-/5Phos/TAGTCCCTTAAGCGGAG/3SpacerC3/-3′). The 5′ phosphate modification of the linker-oligonucleotide aids ligation of the linker, and the C3spacer modification at the 3′ end of the linker-oligonucleotide prevents priming of *Taq* polymerase. Ligations were performed using high concentration T4 ligase (NEB) at room temperature for 2–3 h. After ligation digest with EcoRV to prevent amplification of the internal proviral fragment, primary PCR was performed using high-fidelity Platinum *Taq* (Invitrogen) and the linker primer 5′-GTAATACGACTCACTATAGGGCTCCG-3′ and MuLV LTR3 5′-GCTAGC TTGCCAAACCTACAGGTGG-3′. Cycle conditions were as follows: 94 °C for 2 min, 94 °C for 15 s, 60 °C for 30 s and 72 °C for 1 min for 25 cycles followed by a final extension at 72 °C for 5 min. Primary PCR products were then diluted 1:50 in H$_2$O, and a 2-µl aliquot of the dilution was used for secondary PCR. Secondary PCR was performed using the nested linker primer 5′-AGGGCTCCGCTT

AAGGGAC-3′ and MuLV LTR1 5′-CCAAACCTACAGGTGGGGTCTTTC-3′. Cycle conditions for secondary PCR were identical to the primary PCR. Secondary PCR products were purified using a Qiagen column (QIAquick PCR purification). A 3-µl aliquot of each sample was then ligated into the pCR-Blunt vector (Invitrogen) using high-concentration T4 ligase (NEB) and transformed into TOP10 cells (Invitrogen). Colonies were selected on kanamycin plates containing x-gal for blue–white screening. Ninety-six white colonies were picked from each sample, prepared for sequencing using the Qiagen DirectPrep 96 well kit and sequenced using the M13F(−20) primers. Using methods previously described, we compared retroviral integration sites against the public mouse genome database and identified annotated candidate genes located near each retroviral integration site. All sequences and tumour integration profiles will be deposited into the Retrovirus Tagged Cancer Gene Database (RTCGD).

Lentiviral shRNA RasGRP1 construct and infection. pSicoR-RasGRP1 shRNA-puro-t2a-EGFP was constructed by phosphorylating and annealing primers sh-sense-RasGRP1 5′-TGATCGCTGCAAGCTTTCCATTCAAGAGAT GGAAAGCTTGCAGCGATCTTTTTTC-3′ and sh-antisense-RasGRP1 5′-TCG AGAAAAAAGATCGCTGCAAGCTTTCCATCTCTTGAATGGAAAGCTTGCA GCGATC-3′ and ligating the mixture to Hpa1/Xho1-digested pSicoR-puro-t2a-EGFP. This is designed to target base pair 1503 in mouse *Rasgrp1*. Control vector is pSicoR-puro-t2a-EGFP. 293T cells were plated to a density of 4 million 24 h before transfection. FuGENE 6 transfection reagent was used with 1.5 µg each of packaging plasmids pRSV-Rev, pMDLg-RRE, the envelope pVSV-G and 6 µg of pSicoR-RasGRP1 shRNA-puro-t2a-EGFP or pSicoR-puro-t2a-EGFP. After 72 h, supernatant was collected and concentrated at 25,000 r.p.m. in an ultracentrifuge for 1.5 h and brought to a final volume of 100 µl. Concentrated lentivirus was allowed to re-suspend overnight at 4 °C.

Bone marrow cells were harvested and kept in cytokine-rich media from 2 to 10 days before transduction. Three hundred and fifty thousand cells were plated, treated with polybrene and transduced with 30 µl of concentrated virus. Plates were spin-infected for 2 h, moved to an incubator for 2 h, and virus-containing supernatant was removed and cells placed in fresh cytokine-enriched media for 48 h before FACS analysis for GFP. GFP-positive cells were collected on an Aria sorter and plated in methylcellulose containing MEK inhibitor and GM-CSF 10 ng ml^{-1} at consistent cell numbers in each independent experiment (range 1,200–15,000 cells per condition). Colony number was quantified after 8 days in methylcellulose.

Quantitative rtPCR. Quantification of proviral insertions was performed on DNA isolated from leukaemia mice and normalized for DNA quality based on threshold cycle of amplification of a control DNA region. The samples were amplified in an ABI Prism 7700 sequence detection system. The ΔC_t was calculated for each sample and compared with sensitive leukaemias as using the $\Delta\Delta C_t$ method. Fold increase or decrease was calculated using the $2^{-\Delta\Delta C_t}$. RNA was extracted using Qiagen RNeasy kit and cDNA was synthesized using the Superscript First-Strand Synthesis system for rtPCR (Invitrogen). GAPDH expression was measured in each sample to standardize each reaction. Fold increase or decrease was calculated using the $2^{-\Delta\Delta C_t}$.

Statistical analysis. Statistical analysis and graphs were generated using Prism 4 (GraphPad software). Survival curves were created using the product limit method of Kaplan and Meier, and compared using the log rank test (Mantel–Haenszel test) with a two-tailed *P* value. Colony growth was evaluated as percentage maximum growth ((average colony number in two replicate plates)/(average colony number in plates 0.2% DMSO) × 100). Mean percentage maximum growth was analysed with error bars representing the s.e.m. for independent samples. The significance of experimental results was determined by the Student's *t*-test unless otherwise noted. IC$_{50}$ values and 95% CI were calculated using nonlinear fit – log inhibitor versus normalized response variable slope program in Prism 5 software.